

# Power-grid stability prediction using transferable machine learnings

Seong-Gyu Yang (양성규),<sup>1,2</sup> Beom Jun Kim (김범준),<sup>2</sup> Seung-Woo Son (손승우),<sup>1,3, a)</sup> and Heetae Kim (김희태)<sup>4,5, b)</sup>

<sup>1)</sup>Asia Pacific Center for Theoretical Physics, Pohang 37673, Republic of Korea

<sup>2)</sup>Department of Physics, Sungkyunkwan University, Suwon 16419, Republic of Korea

<sup>3)</sup>Department of Applied Physics, Center for Bionano Intelligence Education and Research, Hanyang University, Ansan 15588, Republic of Korea

<sup>4)</sup>Department of Energy Technology, Korea Institute of Energy Technology, Naju 58330, Republic of Korea

<sup>5)</sup>Instituto de Data Science, Universidad del Desarrollo, Santiago 7610658, Chile

(Dated: 15 October 2021)

Complex network analyses have provided clues to improve power-grid stability with the help of numerical models. The high computational cost of numerical simulations, however, has inhibited the approach especially when it deals with the dynamic properties of power grids such as frequency synchronization. In this study, we investigate machine learning techniques to estimate the stability of power grid synchronization. We test three different machine learning algorithms—random forest, support vector machine, and artificial neural network—training them with two different types of synthetic power grids consisting of homogeneous and heterogeneous input-power distribution, respectively. We find that the three machine learning models better predict the synchronization stability of power-grid nodes when they are trained with the heterogeneous input-power distribution than the homogeneous one. With the real-world power grids of Great Britain, Spain, France, and Germany, we also demonstrate that the machine learning algorithms trained on synthetic power grids are transferable to the stability prediction of the real-world power grids, which implies the prospective applicability of machine learning techniques on power-grid studies.

**The increasing capacity of renewable power generation brings about frequent fluctuations in a power grid’s operational frequency, which consequently threatens the power-grid stability. Thus, it is becoming more important to keep the power system controlled as well as to predict its stability. In this paper, we aim at the prediction of the synchronization recovery of power-grid nodes using machine learning techniques. As large data sets to train machine learning models, we first generate synthetic power grids<sup>1</sup>. We find that three machine learning models—random forest, support vector machine, and artificial neural network—well predict the stability of the synthetic power-grid nodes. Furthermore, we successfully apply the machine learning algorithms to the stability analysis of real power grids<sup>2,3</sup>—British, French, Spanish, and German power grids—and find that our models are transferable to different power-grid structure with various system size.**

ity of power grids in terms of the phase and frequency dynamics of power grids. The dynamics of an alternating current (AC) power system is described by the second-order Kuramoto model<sup>16–18</sup>. Accordingly, the stability evaluation of power systems considering the dynamics of AC power has been studied rigorously in recent works<sup>2,19–28</sup>.

The dynamic model of an AC power system enables us to estimate its stability of the system through numerical simulations. However, its large computational cost comes back to effect negatively the stability evaluation of power systems. It is because the stability depends not only on the network topology<sup>29–33</sup> but also on the parameters related to the dynamics of AC power<sup>21,22,24,34</sup> that require multiple combinations of various test sets. Thus, the estimation of the power-grid stability exploring the parameter space is a challenging problem, for which we have tried to apply machine learning (ML) techniques.

Recently, ML approaches have been used in various fields of physics to reduce the computational costs. For example, the Monte Carlo simulations of glass systems<sup>35</sup> and molecular dynamics simulation<sup>36</sup> have been boosted with a ML technique. ML is also applied in the prediction of nonlinear dynamic systems<sup>37–40</sup>. Rodrigues *et al.* have shown that the applicability of ML techniques to predict the size of epidemic outbreaks and the final state of the coupled oscillator system from the given network topologies and initial conditions<sup>40</sup>.

Although ML is one of the effective methods achieving breakthroughs in many problems, it has some drawbacks when applied to the stability prediction of power grids. One drawback is the large-size data set that is essential to properly train ML models. Although there are several open data sets of real-world power grids<sup>3,41–44</sup>, the size and type of power-grid data are still limited. Moreover, when ML models are trained on a specific power-grid topology, they become too optimized

## I. INTRODUCTION

The increasing of renewable capacities can destabilize a power grid due to the high dependency of renewable energy sources on external dynamic factors such as weather conditions<sup>4,5</sup>. Previous studies have focused on the topological properties of power grids<sup>6–9</sup> and their structural vulnerability<sup>8–15</sup>. However, it is also required to estimate the stabil-

<sup>a)</sup>Electronic mail: sonswoo@hanyang.ac.kr

<sup>b)</sup>Electronic mail: heetaekim@udd.cl

(over-fitted) to the topology, so that they are hardly applicable to the other power-grid topologies. These limitations, deficient open data sets and high dependency due to the training on a single power-grid topology, are a challenge to develop transferable ML models which can predict the power-grid stability on any given topology.

In the present paper, we investigate the applicability and transferability of ML algorithms to predict the power-grid stability. We investigate three different ML algorithms—random forest, support vector machine, and artificial neural network—to predict whether a power grid recovers its synchronous state against random perturbations or not. First, we construct the training data sets numerically simulating the synthetic power grids that are generated from the random growth model of power grids<sup>1</sup>. Two different power distribution scenarios—*homogeneous* (HOM) and *heterogeneous* (HET)—are also introduced to estimate the performance of ML algorithms for the different levels of complexity. After constructing the training data sets, in the ML training step, we choose six topological features and three dynamical features to train the transferable ML models<sup>40</sup>. After we train the ML models on the synthetic power grids with the power distributions, we apply the ML models to predict the stability of the real-world power grids—British, French, Spanish, and German—which have different network topologies with different system sizes.

This paper is organized as follows: In Sec. II A, we present the dynamic model of AC power systems which is the second-order Kuramoto type. The details of the three ML algorithms (Sec. II B) and input features (Sec. II C) follow. It is described in Sec. II D how we construct the training data set using the random growth model, and the description of the test data sets for real power grids is given in Sec. II E. We report the prediction performance of our ML models for the training data set and for the test data sets in Sec. III followed by the conclusion and discussions of this paper.

## II. METHODS

### A. Dynamic model of AC power systems: the second-order Kuramoto model

The synchronous phase dynamics of the AC power-grid system is usually described by the following second-order Kuramoto model, which is derived from the energy conservation law in power-grid systems<sup>16–18,45</sup>,

$$\begin{aligned}\dot{\theta}_i &= \omega_i, \\ \dot{\omega}_i &= P_i - \alpha_i \omega_i + \sum_j K_{ij} \sin(\theta_j - \theta_i),\end{aligned}\quad (1)$$

where  $\theta_i$  is the phase angle variable and  $\omega_i$  is the angular frequency of node  $i$  in the reference frame of the rated frequency. The energy dissipation term is written as a multiplication of  $\omega_i$  and the damping coefficient  $\alpha_i > 0$ .  $K_{ij}$  denotes the coupling strength between nodes  $i$  and  $j$  which corresponds to the electric capacity of transmission line between nodes  $i$  and  $j$ .  $P_i$  is the amount of net power production in node  $i$ , which is positive (negative) if the node  $i$  is a producer (consumer). For

energy conservation of the whole system, the total net power production over the networks should be zero, i.e.,  $\sum_i P_i = 0$ . Different from the conventional Kuramoto model, the angular frequency  $\omega_i$  plays as an indicator of synchronization to the rated frequency of the power-grid system. The zero angular frequency for all nodes denotes that the whole system reaches to the synchronization of rated AC frequency.

### B. Three ML algorithms

We design the stability prediction from random perturbations as the binary classification problem. Then we use three ML algorithms to predict the stability of synthetic power grids. One is random forest (RF) which uses the ensemble of decision trees<sup>46,47</sup>, the second is support vector machine (SVM) which is the method to find a hyper plane separating the data points into differently labeled groups in data space<sup>48,49</sup>, and the last is artificial neural network (NN) which is introduced by mimicking the neuron connection<sup>50–52</sup>. Those ML algorithms are the three of basic and frequently used classification algorithms<sup>50,52</sup> and we use all the three in this paper.

For RF, we use 500 different decision trees and each decision tree is trained with a different bootstrap data sample<sup>46,50</sup>. We use the Gaussian radial basis function kernel for SVM<sup>49,50</sup> which is the method to make the hyper plane nonlinear in the input feature space. The NN model consists of an input layer with a bias node, three hidden layers of  $20 \times 20 \times 10$  structure with dropout rate 0.1, and an output layer<sup>50–52</sup>. Rectified linear unit (ReLU) activation function in the hidden layers and the softmax activation function in the output layer are applied. We use the binary cross entropy as the objective function<sup>50,52</sup> and Adam optimizer<sup>53</sup> to find the minimum value of the objective function. We utilize the python scikit-learn package<sup>50,54,55</sup> to construct RF and SVM models and the pytorch package<sup>56,57</sup> to build NN models.

### C. Input features

Power grid stability depends not only on the AC dynamics of voltage but also on the network topology of power producers and consumers<sup>20–22,30,33</sup>. Thus, we choose three dynamic features—net power production ( $P$ ), phase perturbation ( $\theta_{\text{pert}}$ ), and frequency perturbation ( $\omega_{\text{pert}}$ )—with six topological features—degree ( $k$ ),  $k$ -core (core), eigenvector centrality (EC), closeness centrality (CC), betweenness centrality (BC)<sup>58,59</sup>, and companionship inconsistency (CoI)<sup>33,60</sup>—as input features of the ML model training.

The degree of a node  $k$  is the number of its neighbor. The  $k$ -core denotes the largest subnetwork where each node has degree  $k$  at least and a node has the core value of  $k$  if the node belongs to the  $k$ -core but does not to  $(k+1)$ -core. In the previous study, Yang *et al.* showed that the core assigned in a transmission line has a high correlation with the vulnerability of that line in the US-South Canada power grid<sup>32</sup>. The EC

measures the importance of each node related to the eigenvector  $\vec{x}$  corresponding to the largest eigenvalue  $\lambda$  of the network adjacency matrix  $\mathbf{A}$ , i.e.,

$$\mathbf{A}\vec{x} = \lambda\vec{x}. \quad (2)$$

The  $i$ th component of  $\vec{x}$  gives the EC of node  $i$ . The CC of node  $i$  is the reciprocal of the average shortest path length from the node  $i$  to other nodes such that

$$\text{CC}_i = \frac{N-1}{\sum_{j \neq i} d_{ij}}, \quad (3)$$

where  $N$  is the system size and  $d_{ij}$  is the network distance between nodes  $i$  and  $j$ . The BC of node  $i$  measures how many times the node  $i$  lies on the shortest path between all pairs of other nodes in the network,

$$\text{BC}_i = \sum_{j,l} \frac{s'_{jl}(i)}{s_{jl}}, \quad (4)$$

where  $s_{jl}$  is the number of shortest paths between nodes  $j$  and  $l$  and  $s'_{jl}(i)$  is the number of the shortest paths between nodes  $j$  and  $l$  which pass through node  $i$ . The nodes connecting two different groups or clusters usually have the high BC values. The CoI of node  $i$  measures the level of inconsistency while the node  $i$  belongs to a community<sup>33,60</sup>. In the Chilean power grid, nodes having low CoI value tend to have a wide basin stability transition window, which can be utilized as an indicator of the system failure<sup>33</sup>. The degree  $k$  and the dynamical features have local information of each node but the other topological measures reflect the global information of power-grid topology.

#### D. Training on synthetic power grids

We generate synthetic power grids consisting of  $N = 500$  nodes using a random growth model in the Ref. 1. We choose the same parameters which are used to generate power grids similar to the Western US power grid in topological properties. In each synthetic power grid, we assign two different power distributions. (i) *Homogeneous* (HOM) distribution: randomly chosen  $N/2 (= 250)$  nodes are assigned as producers ( $P_i = +1$ ) and the other half as consumers ( $P_i = -1$ ). The absolute value of net power production is homogeneous as  $|P_i| = 1$  for all nodes. (ii) *Heterogeneous* (HET) distribution: randomly chosen  $N/10 (= 50)$  nodes are the large producers (consumers) with net power production  $P_i = 2(-2)$  and other  $2N/5 (= 200)$  nodes are the small producers (consumers) having  $P_i = 0.2(-0.2)$ . In the HET distribution, we consider a few large producers/consumers and many small producers/consumers, which is more similar to real power grids than the HOM distribution.

On the generated synthetic power-grid structure, we numerically integrate Eq. (1) using the 4th-order Runge-Kutta method with the integration time step size  $\Delta t = 10^{-3}$  for  $5 \times 10^5$  time steps. The coupling strength for every connected pairs of nodes  $i$  and  $j$  is chosen as  $K_{ij} = K = 10$  which is large enough. The damping parameter is  $\alpha_i = \alpha = 0.1$  for all nodes.

After the power grid reaches a synchronous state, we perturb the state of node  $i$  changing its phase and angular frequency  $(\theta_i, \omega_i)$  to the new state  $(\omega_{\text{pert}}, \theta_{\text{pert}})$  which are randomly chosen from the uniform distribution in the range of  $[-50, 50] \times [-\pi, \pi]$ . We apply 10 random perturbations on each node, and then put the label for each trial as '+1' if the system recovers its synchronous state from the given perturbation or '-1' for the opposite cases.

The training data sets consist of nine input features and the label of '+1' or '-1' which denotes whether the system recovers from the given perturbation or not. We divide the whole data sets on the synthetic power grids into training (60%), validation (20%), and test data set (20%) for NN models, and training (80%) and test data set (20%) for RF and SVM models. We train and validate the ML models with training and validation data sets respectively, and estimate the prediction performance with the test data set. The performance measures of the ML models on synthetic power grids are presented in Sec. III A.

#### E. Real power grid data

To test the transferability of our ML models, we prepare the test data sets for different power-grid topologies in the real world. We utilize the open public data set of British, Spanish, French, and German power grids for the network structures<sup>2,3</sup>. Figure 1 displays the four European power grids, where the yellow circles denote the consumers and green rhombi denote the producers. The system sizes of the real power grids are different and their structures show different features.

The power generation and consumption information of each node is not available for British, Spanish, and French power grids. Thus, we randomly assign the net power production  $P_i$  for each node with two power distributions which are used in the synthetic power grids (details in Sec. II D). The system sizes of three European power grids are  $N_{\text{GB}} = 120$  (Great Britain),  $N_{\text{FR}} = 146$  (France), and  $N_{\text{ES}} = 98$  (Spain). For three European power grids, we assign the same value as in Ref. 2 to the transmission capacity  $K$ . With the damping parameter  $\alpha = 0.1$ , we numerically integrate Eq. (1) on each power grid. If the system doesn't reach the synchronous state, we newly distribute the net power production  $P$  for every node and integrate Eq. (1) again until the system becomes stable.

For the German power grid, the net power production data of each node are available in the ELMOD-DE data set<sup>3</sup>. We utilize the net power production data to simulate German power grid. The system size of German power grid is  $N_{\text{DE}} = 438$ . The net power production of node  $i$  is determined as

$$P_i = \gamma C_i - D_i + I_i - E_i, \quad (5)$$

where  $C_i$  is the maximum power generation capacity of power plant node  $i$ ,  $D_i$  is the power demand of node  $i$ , and  $\gamma$  is the operation rate of power plants which is fixed as  $\gamma = 0.4$  in our simulation.  $I_i(E_i)$  is the annual average of power import (export) of node  $i$  which has cross-border transmission line. In the ELMOD-DE raw data<sup>3</sup>, there are hourly power import

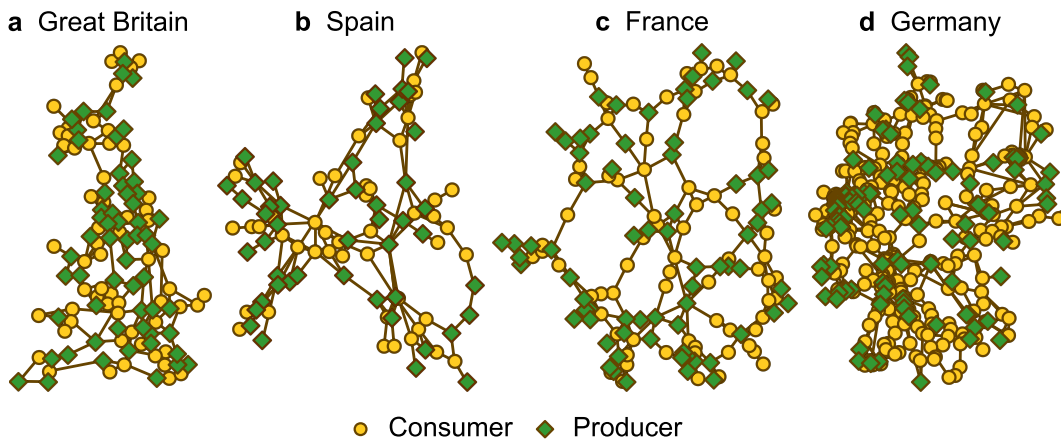


FIG. 1. **Network topologies of four European power grids.** The yellow circles (green rhombi) denote the consumers (producers). The network sizes of real power grids are  $N_{GB} = 120$ ,  $N_{ES} = 98$ ,  $N_{FR} = 146$ , and  $N_{DE} = 438$ . **a-c** For British, French, and Spanish power grids, we generate the power grids with the power distributions used in the synthetic power grid generation due to the absence of the power generation and consumption data. **d** For the German power grid, we utilize the real power generation and consumption data which are included in the open data set of ELMOD-DE. In the German power grid, 113 nodes are producers and 325 nodes are consumers.

and export data for a year in the unit of electric energy (GWh) and we change them in the unit of electric power (GW) averaging the annual data and dividing them by 3600 seconds. For the power balance, i.e.,  $\sum_i P_i = 0$ , we distribute the net power demand equally to the other nodes where the net power production is zero. Differently from Ref. 26, we consider the power generation not only from fossil fuels but also from the renewable energy sources including run-of-river, biomass, geothermal, photovoltaic, onshore and offshore wind power. We also consider the annual average power import and export near country borders. We find the minimum  $K$  in which the power grid operates stably and fix all electric capacity of transmission lines as  $K = 0.49$  ( $\approx 0.62$  GW). Even for the minimum  $K$  we find, the average basin stability of German power grid shows a high value of 0.869. We adequately rescale all variables to dimensionless quantities<sup>16,45</sup> using the damping parameter  $\alpha = 0.1$  and the angular momentum of rotors rotating in rated frequency of 50 Hz. We assume that each node's moment of inertia is  $40 \times 10^3 \text{ kg m}^2$  which corresponds to the inertia of rotors in 400 MW power plants<sup>26,31</sup>.

After the system reaches the synchronous steady state, we apply 50 random perturbations to each node on the real power-grid topologies and collect the results of recovery from the perturbations. The real power grids deliver the electric power stably as designed, thus the power grids show high basin stability. Thus, we do not make the number of positively and negatively labeled data equal. All data points are used to estimate the performance of our ML models on the real power grids. The results on the real power grids are presented in Sec. III B.

### III. RESULTS

#### A. Synthetic power grids

We evaluate the performance of our ML models with the  $F_1$  score which is the harmonic mean of sensitivity and precision. The sensitivity and precision are the predictive performance measures of ML. The sensitivity (also known as 'recall') is defined as the ratio of the true positive and positively labeled data points; the precision, true positive and positive predictions. We present the  $F_1$  score of our ML models for

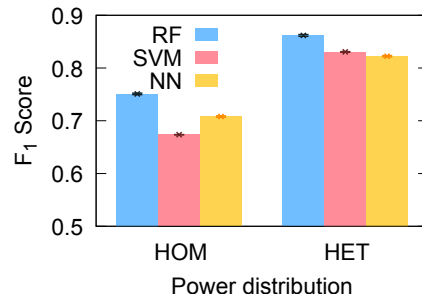


FIG. 2. **Average  $F_1$  score for synthetic power grids with two different power distributions.** The blue bars denote the average  $F_1$  score for the random forest (RF) models, pink bars for the support vector machine (SVM), and yellow bars for the artificial neural network (NN). Three ML models trained with the HET distribution show higher  $F_1$  score value than those trained with the HOM distribution. Among the three ML models, the RF model shows better performance than the others, thus the RF model trained with the HET distribution is the best among three approaches in the synthetic power grids. The average  $F_1$  score for all cases have higher value than the random prediction score 0.5. The  $F_1$  score is averaged over 10 randomly sampled data sets.

	HOM	RF	SVM	NN
Accuracy	0.756(2)	0.682(1)	0.711(1)	
Sensitivity	0.732(2)	0.654(1)	0.699(3)	
Precision	0.779(3)	0.693(1)	0.716(2)	
Specificity	0.781(4)	0.710(1)	0.732(3)	
Negative Predictive Value	0.744(1)	0.672(1)	0.706(2)	

	HET	RF	SVM	NN
Accuracy	0.856(3)	0.827(1)	0.815(1)	
Sensitivity	0.893(5)	0.848(2)	0.854(9)	
Precision	0.832(7)	0.813(1)	0.793(6)	
Specificity	0.81(1)	0.806(1)	0.77(1)	
Negative Predictive Value	0.886(4)	0.841(2)	0.843(7)	

TABLE I. **Other machine learning performance measures for synthetic power grid.** The accuracy, sensitivity, precision, specificity, and negative predictive value for machine learning prediction on the synthetic power grids. All the measures are averaged over 10 differently sampled test data sets. The all measures show better performance for the *heterogeneous* (HET) distribution than for the *homogeneous* (HOM) distribution.

the HOM and HET power distributions on synthetic power grids in Fig. 2. All measures are averaged over 10 different training data sets. In Fig. 2, the  $F_1$  score is higher than 0.6 for both power distributions and three different ML models, which means that the ML prediction shows better performance than random. Prediction in the HET distribution performs better than that in the HOM, and the RF shows the best performance among the three ML models.

The other performance measures—accuracy, sensitivity, precision, specificity, and negative predictive value—are summarized in Table I. The accuracy is defined by the ratio with the number of truly predicted data points and the size of data sets. The specificity (negative predictive value) corresponds to the sensitivity (precision) for the prediction of negatively labeled data. Sensitivity and precision are the performance measures for the prediction of system recovery, and the specificity and the negative predictive value for the system failure. All performance measures in Table I also show that the ML models work better than the random prediction for both power distributions. Again, the trained models with the HET distribution show better performance than those with the HOM distribution.

We next investigate the feature importance between nine input features measuring the permutation importance to glimpse how the ML models utilize the features. The permutation importance enables us to estimate the dependency on each feature in the machine prediction<sup>61</sup>. The permutation importance for an input feature is the decrease of the accuracy when the value of the feature is randomly shuffled. The random shuffling of the feature value breaks the correlation between the feature and the label, but the distribution of the feature is kept unchanged. The permutation importance for all features is normalized to make the sum to unity to estimate the relative importance. Figure 3 shows the permutation importance of nine input features for two different power distributions on the synthetic power grid. The result shows that the ML mod-

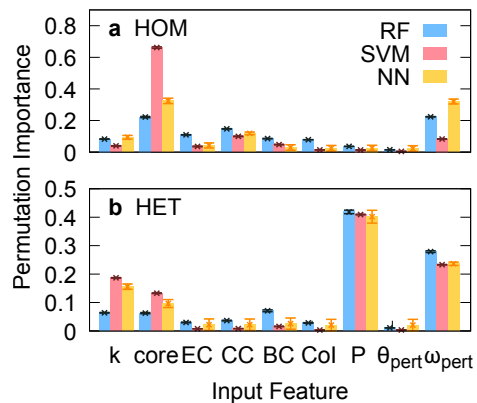


FIG. 3. **Permutation importance on the machine predictions of synchronization recovery from random perturbations.** The feature importance for machine learning models trained with **a** homogeneous (HOM) and **b** heterogeneous (HET) power distributions. The blue bars denote the average permutation importance for random forest (RF) models, pink bars for support vector machine (SVM), and yellow bars for artificial neural network (NN). The permutation importance for all input features is averaged over 10 different sampled data sets.

els depend on both the dynamical and topological features. For the ML models trained on the HOM distribution, they depend highly on core and  $\omega_{\text{pert}}$  more than other features. SVM shows a much stronger dependency on core than other predictions (Fig. 3a). The ML models trained with the HET distribution also show high dependency on  $\omega_{\text{pert}}$ . However, they show a much stronger dependency on the net power production  $P_i$  (Fig. 3b). We believe that the perturbation applied on a node with large  $P$  has a larger effect on the whole system than on a node with small  $P$  and the result is reflected on the machine predictions.

## B. Real power grids

On the synthetic power grids, we train the ML model, and predict the synchronization stability estimating the prediction performance of the models. However, applying the ML models, which are trained on synthetic power grids, to predict the stability of real power grids is another problem. Even though the ML models work well on the data sets which are used in the training, the machine is not guaranteed for the different problems, in this case different power grids of the real world, for example. This is the machine ‘transferability’ issue—whether a ML model is transferable to different, yet similar problems. In this section, we test and verify the transferability of our ML models, applying them to stability prediction of real power grids.

### 1. Three European power grids

We simulate the British, Spanish, and French power grids with two power distributions which are used in synthetic

Great Britain	HOM			HET		
	RF	SVM	NN	RF	SVM	NN
Accuracy	0.559(4)	0.544(4)	0.554(2)	0.865(2)	0.854(2)	0.869(9)
Sensitivity	0.809(6)	0.730(6)	0.806(4)	0.931(3)	0.892(3)	0.92(2)
Precision	0.549(3)	0.543(3)	0.546(1)	0.907(1)	0.928(2)	0.915(2)
Specificity	0.292(4)	0.344(5)	0.286(4)	0.549(5)	0.673(7)	0.59(2)
Negative Predictive Value	0.589(9)	0.545(6)	0.579(3)	0.630(8)	0.569(7)	0.66(4)

Spain	HOM			HET		
	RF	SVM	NN	RF	SVM	NN
Accuracy	0.633(4)	0.523(2)	0.838(6)	0.840(3)	0.825(2)	0.874(4)
Sensitivity	0.602(5)	0.464(3)	0.90(1)	0.882(4)	0.869(2)	0.961(6)
Precision	0.964(3)	0.977(1)	0.911(3)	0.917(1)	0.912(6)	0.892(2)
Specificity	0.847(1)	0.926(3)	0.39(3)	0.659(5)	0.639(4)	0.498(9)
Negative Predictive Value	0.236(3)	0.200(1)	0.38(2)	0.565(7)	0.530(3)	0.76(3)

France	HOM			HET		
	RF	SVM	NN	RF	SVM	NN
Accuracy	0.735(3)	0.700(4)	0.757(1)	0.867(4)	0.845(2)	0.882(6)
Sensitivity	0.783(4)	0.671(4)	0.875(1)	0.880(5)	0.845(3)	0.894(8)
Precision	0.854(3)	0.908(1)	0.816(1)	0.965(2)	0.976(1)	0.970(2)
Specificity	0.586(9)	0.790(2)	0.390(2)	0.765(9)	0.844(3)	0.795(9)
Negative Predictive Value	0.466(5)	0.436(4)	0.503(2)	0.461(8)	0.421(4)	0.503(2)

TABLE II. **Other machine learning prediction performance measures for three European power grids.** Five different performance measures averaged over 10 machine learning models trained on different test sets for three algorithms on three European power grids. All measures show better performance for the *heterogeneous* (HET) distribution than for the *homogeneous* (HOM) distribution. Furthermore, the prediction performance for positively labeled data is much better than that for negatively labeled data.

power grid generation and build the test data sets for three European power grids (details in Sec. II E). The ML mod-

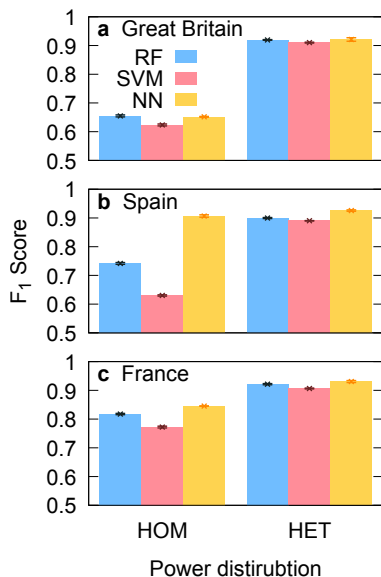


FIG. 4. **Average F<sub>1</sub> score for the machine prediction on three European power grids.** Machine learning performance estimated as the F<sub>1</sub> score for three European power grids. Like in the synthetic power grids, the machine predictions for *heterogeneous* (HET) power distribution show better performance than for *homogeneous* (HOM) distribution.

els trained on the synthetic power grids and each power distribution are applied to predict the results from random perturbations on the real power grids which are generated with the same power distribution. Figure 4 shows the averaged F<sub>1</sub> score of the ML models on three European power grids for each power distribution. We also measure the other performance measures for three European power grids and the results are presented in Table II. As in the synthetic power grids, machine predictions for the HET distribution show better performance than those for the HOM distribution. However, the performance measures for negatively labeled data tend to have small value than estimations for positively labeled data. It means that the ML models predict the recovery of synchronous state better than the failure of power systems.

## 2. German power grids

Since there exists open power production data for the German power grid<sup>3</sup>, we utilize them and build the test data set for the German power grid (details in Sec. II E). After the test data set for German power grid is prepared, we predict whether the system recovers the synchronous state from the given perturbations with the ML models trained on the synthetic power grid. The ML models trained with two different power distributions are applied to predict the results for the same power grid. Figure 5 shows the F<sub>1</sub> score of the models and all ML models show better prediction performance than the random prediction even when the power distribution of the German power grid is different from the training data set of synthetic

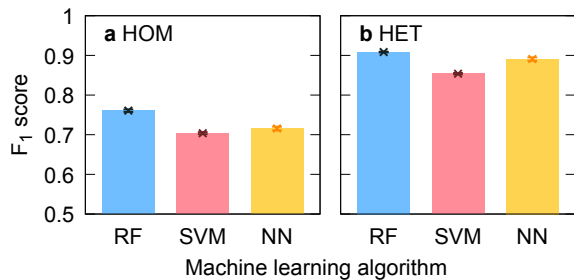


FIG. 5.  $F_1$  score of three different machine learning models trained with *homogeneous* (HOM) and *heterogeneous* (HET) power distribution for German power grid. Three different machine learning algorithms—random forest (RF), support vector machine (SVM), and artificial neural network (NN)—trained on synthetic power grids show high prediction performance.

HOM	RF	SVM	NN
Accuracy	0.625(4)	0.558(3)	0.572(6)
Sensitivity	0.685(5)	0.604(4)	0.620(7)
Precision	0.854(1)	0.842(2)	0.846(1)
Specificity	0.227(6)	0.252(5)	0.254(6)
Negative Predictive Value	0.098(2)	0.088(2)	0.092(2)

HET	RF	SVM	NN
Accuracy	0.841(2)	0.761(3)	0.812(7)
Sensitivity	0.904(3)	0.800(4)	0.881(9)
Precision	0.912(1)	0.914(1)	0.900(2)
Specificity	0.423(7)	0.502(4)	0.35(2)
Negative Predictive Value	0.402(5)	0.276(3)	0.31(1)

TABLE III. **Other machine learning prediction performance measures for German power grid.** The averaged accuracy, sensitivity, precision, specificity, and negative predictive value for machine learning prediction on the synthetic power grids of two different power distributions. HOM and HET denote *homogeneous* and *heterogeneous* power distributions respectively. The specificity (negative predictive value) is the negative prediction version of sensitivity (precision).

power grid. Compared with the  $F_1$  score for the HOM distribution, the prediction for the HET distribution shows superior performance. The other performance measures for the HET distribution also have higher values than those for the HOM distribution (see Table III). Furthermore, the performance measures for positively labeled data have much higher value than those for negatively labeled data similarly to our observation for three European power grids.

Based on the predictability of our ML model for the recovery of synchronous state from nodal perturbations, we extend the prediction of the stability of the whole power grid which can be estimated from the average basin stability. The average basin stability is the average of single-node basin stability<sup>62,63</sup> for all nodes in German power grid, and we measure the machine prediction of average basin stability as the rate of positively predicted data. In Table IV, we present the average basin stability of German power grids and the predictions of our ML model. The ML predictions are averaged over 10

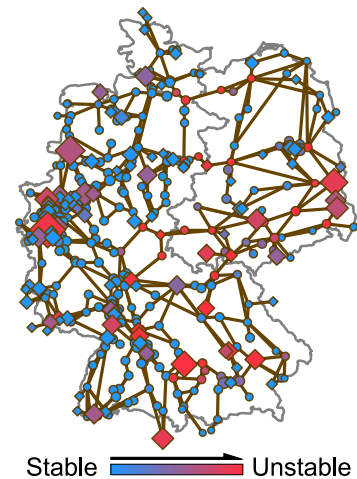


FIG. 6. **Basin stability of each node in German power grid.** The rhombi (circles) denote the net producers (consumers). The size of each node is proportional to its net power production and the color of node indicates the single-node basin stability estimated from 50 random perturbations. Nodes which have large net power production tend to be more unstable than others of small net power production. Furthermore, nodes which have transmission line across the inner German border tend to be more unstable than the other nodes with similar net power production value.

	RF	SVM	NN
HOM	0.697(5)	0.623(3)	0.636(6)
HET	0.862(2)	0.761(3)	0.851(9)
Average basin stability	0.869		

TABLE IV. **Machine prediction of average basin stability of German power grid.** The average basin stability of German power grid is estimated by averaging all nodes' single-node basin stability and it is 0.869. The machine prediction of basin stability is the rate of data which is predicted to be recover synchronization from given perturbation. HOM denotes the *homogeneous* and HET denotes the *heterogeneous* power distribution. The RF prediction under the HET distribution shows the best performance.

different models trained with 10 sampling data sets. The machine predictions of basin stability are 0.697, 0.623, and 0.636 under the HOM power distribution and 0.862, 0.761 and 0.851 under the HET distribution for RF, SVM, and NN models respectively. The average basin stability also shows that the RF prediction under the HET distribution performs the best.

#### IV. CONCLUSION AND DISCUSSIONS

In this work, we have investigated the applicability of ML techniques to predict the power-grid stability developing transferable ML models. The transferable ML models (RF, SVM, and NN) are trained on synthetic power grids using both topological and dynamical features. The synthetic power grids were generated with the random growth model<sup>1</sup>, and we assigned two different power distributions, the HOM

and HET distributions, to the training data sets. The performances of our ML models have been estimated with average accuracy, sensitivity, precision, specificity, negative predictive value, and mainly the  $F_1$  score. All ML models have shown high predictive performance for both power distributions achieving the  $F_1$  score higher than 0.65. Especially the RF models trained with the HET distribution have shown the best performance of  $F_1$  score higher than 0.85 for the synthetic power grids. We have tried to understand how our ML models work by measuring the permutation importance and we have found that both topological and dynamical features play an important role in machine prediction. The core is the most important feature in the predictions for the HOM power distribution, and the net power production plays the most important role in the prediction performance for the HET distribution.

We have also estimated the prediction performance of transferable ML models on real power grids with the performance measures and especially with the  $F_1$  score. We have simulated four European power grids including Great Britain, France, Spain, and Germany and constructed the test data sets for the real power grids. Surprisingly, even though our models are trained on synthetic power grids, the models have shown high prediction performance on real power grids. Comparing two power distributions, the ML models trained with the HET distribution performed better than those with the HOM distribution. We believe that the HET distribution is much more similar to the real net power distribution than the HOM distribution, and it makes the prediction of ML models trained with the HET distribution better for real power grids. In addition, all models better predict the recovery of synchronous state from random perturbations showing high value of the sensitivity and the precision than to predict the failure of recovery which is estimated with the specificity and the negative predictive value. For German power grid, the RF models show the highest average  $F_1$  score, but for the other three European countries, NN models show comparable performance with the RF models. The NN models trained with the HOM distribution on the synthetic power grid show the best performance on the Spanish power grid. The machine prediction of whole power grid stability has also been discussed in this paper. We have predicted the overall stability of power grid estimating the average basin stability with our ML models and the RF models trained with the HET distribution give the closest value to the average basin stability obtained from the numerical simulation on German power grid.

Even if the bias in the training data set is removed, the ML models predict better system recovery on the real power-grid topologies than the system failure. This result is obvious in the prediction of the ML models trained with HET distribution. We believe that this property of our ML models is beneficial to apply the ML techniques to real power system control and operation. When power malfunctions occur, the machine predicts the results of the malfunction and alerts the danger. If the machine prediction is recovery, people can have stronger trust in the result. In the opposite case of failure prediction, however, system operators should pay more attention and need to figure out whether the malfunction ultimately leads to the system failure or recovery. In this manner, machine predicts the

safety of the power system conservatively and can help system operators.

The ML techniques have much potential applicability. Power-grid stability prediction can be regarded as a classification problem and the problem is handled as such in this paper. However, the cascading failure of a power system, which is also an important problem in the system stability analysis<sup>2,10,12,23,25,64</sup>, belongs to a different group of problems. The cascading failure is a dynamic phenomenon and this problem should be dealt with other ML techniques because the state of the system changes in time. To deal with such time varying phenomena, the Recurrent Neural Network (RNN) can be a candidate for the ML technique. The typical example of RNN is the reservoir computing method, and the method is used to predict the trajectory of chaotic system recently<sup>37–39</sup>.

## ACKNOWLEDGMENTS

This research was supported by “Human Resources Program in Energy Technology” of the Korea Institute of Energy Technology Evaluation and Planning (KETEP), granted financial resource from the Ministry of Trade, Industry and Energy, Republic of Korea Grant No. 20194010000290 (S.-G.Y. and B.J.K.), the National Research Foundation of Korea through the Grant No. NRF-2020R1A2C2010875 (S.-W.S.), and the Chilean Council of Scientific and Technological Research, CONICYT, through the grant FONDECYT N.11190096 (H.K.). This work was also partly supported by Institute of Information & Communication Technology Planning & Evaluation grant funded by the Korea government (No. 2020-0-01343, Artificial Intelligence Convergence Research Center (Hanyang University)) (S.-W.S.).

## DATA AVAILABILITY

The data that support the findings of this study are available from the corresponding author upon reasonable request.

## REFERENCES

- <sup>1</sup>P. Schultz, J. Heitzig, and J. Kurths, “A random growth model for power grids and other spatially embedded infrastructure networks,” *Eur. Phys. J. Spec. Top.* **223**, 2593 (2014).
- <sup>2</sup>B. Schäfer, D. Witthaut, M. Timme, and V. Latora, “Dynamically induced cascading failures in power grids,” *Nat. Commun.* **9**, 1975 (2018).
- <sup>3</sup>J. Egerer, “Open source electricity model for Germany (ELMOD-DE), technical report no. 83,” <http://www.diw.de/elmod> (2016).
- <sup>4</sup>M. Anvari, B. Werther, G. Lohmann, M. Wächter, J. Peinke, and H.-P. Beck, “Suppressing power output fluctuations of photovoltaic power plants,” *Solar Energy* **157**, 735 (2017).
- <sup>5</sup>H. Haehne, J. Schottler, M. Waechter, J. Peinke, and O. Kamps, “The footprint of atmospheric turbulence in power grid frequency measurements,” *Europhys. Lett.* **121**, 30001 (2018).
- <sup>6</sup>K. Sun, “Complex networks theory: A new method of research in power grid,” in *2005 IEEE/PES Transmission Distribution Conference Exposition: Asia and Pacific* (2005) pp. 1–6.

- <sup>7</sup>P. Hines, S. Blumsack, E. C. Sanchez, and C. Barrows, “The topological and electrical structure of power grids,” in *2010 43rd Hawaii International Conference on System Sciences* (2010) pp. 1–10.
- <sup>8</sup>V. Rosato, S. Bologna, and F. Tiriticco, “Topological properties of high-voltage electrical transmission networks,” *Electr. Power Syst. Res.* **77**, 99 (2007).
- <sup>9</sup>D. H. Kim, D. A. Eisenberg, Y. H. Chun, and J. Park, “Network topology and resilience analysis of south korean power grid,” *Physica A* **465**, 13 (2017).
- <sup>10</sup>P. Crucitti, V. Latora, and M. Marchiori, “Model for cascading failures in complex networks,” *Phys. Rev. E* **69**, 045104 (2004).
- <sup>11</sup>R. Albert, I. Alvert, and G. L. Nakarado, “Structural vulnerability of the North American power grid,” *Phys. Rev. E* **69**, 025103(R) (2004).
- <sup>12</sup>R. Kinney, P. Crucitti, R. Albert, and V. Latora, “Modeling cascading failures in the north american power grid,” *Eur. Phys. J. B* **46**, 101 (2005).
- <sup>13</sup>G. Chen, Z. Y. Dong, D. J. Hill, G. H. Zhang, and K. Q. Hua, “Attack structural vulnerability of power grids: A hybrid approach based on complex networks,” *Physica A* **389**, 595 (2010).
- <sup>14</sup>S. Arianos, E. Bompard, A. Carbone, and F. Xue, “Power grid vulnerability: A complex network approach,” *Chaos* **19**, 013119 (2009).
- <sup>15</sup>S. Pahwa, C. Scoglio, and A. Scala, “Abruptness of cascade failures in power grids,” *Sci. Rep.* **4**, 3694 (2014).
- <sup>16</sup>G. Filatrella, A. H. Nielsen, and N. F. Pedersen, “Analysis of a power grid using a Kuramoto-like model,” *Eur. Phys. J. B* **61**, 485 (2008).
- <sup>17</sup>F. A. Rodrigues, T. K. D. Peron, P. Ji, and J. Kurths, “The Kuramoto model in complex networks,” *Phys. Rep.* **610**, 1 (2016).
- <sup>18</sup>A. Arenas, A. Díaz-Guilera, J. Kurths, Y. Moreno, and C. Zhou, “Synchronization in complex networks,” *Phys. Rep.* **469**, 93 (2008).
- <sup>19</sup>P. Hines, E. C. Sanchez, and S. Blumsack, “Do topological model provide good information about electricity infrastructure vulnerability?” *Chaos* **20**, 033122 (2010).
- <sup>20</sup>H. Kim, M. J. Lee, S. H. Lee, and S.-W. Son, “On structural and dynamical factors determining the integrated basin instability of power-grid nodes,” *Chaos* **29**, 103132 (2019).
- <sup>21</sup>H. Kim, S. H. Lee, and P. Holme, “Building blocks of the basin stability of power grids,” *Phys. Rev. E* **93**, 062318 (2016).
- <sup>22</sup>H. Kim, S. H. Lee, J. Davidsen, and S.-W. Son, “Multistability and variations in basin of attraction in power-grid systems,” *New J. Phys.* **20**, 113006 (2018).
- <sup>23</sup>I. Simonsen, L. Buzna, K. Peters, S. Bornholdt, and D. Helbing, “Transient dynamics increasing network vulnerability to cascading failures,” *Phys. Rev. Lett.* **100**, 218701 (2008).
- <sup>24</sup>M. Rohden, A. Sorge, M. Timme, and D. Witthaut, “Self-organized synchronization in decentralized power grids,” *Phys. Rev. Lett.* **109**, 064101 (2012).
- <sup>25</sup>B. Schäfer and G. C. Yalcin, “Dynamical modeling of cascading failures in the Turkish power grid,” *Chaos* **29**, 093134 (2019).
- <sup>26</sup>H. Tahler, S. Olmi, and E. Schöll, “Enhancing power grid synchronization and stability through time-delayed feedback control,” *Phys. Rev. E* **100**, 062306 (2019).
- <sup>27</sup>X. Zhang, C. Ma, and M. Timme, “Vulnerability in dynamically driven oscillatory networks and power grids,” *Chaos* **30**, 063111 (2020).
- <sup>28</sup>X. Zhang, D. Witthaut, and M. Timme, “Topological determinants of perturbation spreading in networks,” *Phys. Rev. Lett.* **125**, 218301 (2020).
- <sup>29</sup>M. Rohden, A. Sorge, D. Witthaut, and M. Timme, “Impact of network topology on synchrony of oscillatory power grids,” *Chaos* **24**, 013123 (2014).
- <sup>30</sup>J. F. Wienand, D. Eidmann, J. Kremers, J. Heitzig, F. Hellmann, and J. Kurths, “Impact of network topology on the stability of dc microgrids,” *Chaos* **29**, 113109 (2019).
- <sup>31</sup>P. J. Menck, J. Heitzig, J. Kurths, and H. J. Schellnhuber, “How dead ends undermine power grid stability,” *Nat. Commun.* **5**, 3696 (2014).
- <sup>32</sup>Y. Yang, T. Nishikawa, and A. E. Motter, “Small vulnerable sets determine large network cascades in power grids,” *Science* **358**, 6365 (2017).
- <sup>33</sup>H. Kim, S. H. Lee, and P. Holme, “Community consistency determines the stability transition window of power-grid nodes,” *New J. Phys.* **17**, 113005 (2015).
- <sup>34</sup>F. Molnar, T. Nishikawa, and A. E. Motter, “Asymmetry underlies stability in power grids,” *Nat. Commun.* **12**, 1457 (2021).
- <sup>35</sup>B. McNaughton, M. V. Milošević, A. Perali, and S. Pilati, “Boosting Monte Carlo simulations of spin glasses using autoregressive neural networks,” *Phys. Rev. E* **101**, 053312 (2020).
- <sup>36</sup>V. Botu and R. Ramprasad, “Adaptive machine learning framework to accelerate ab initio molecular dynamics,” *International Journal of Quantum Chemistry* **115**, 1074 (2015).
- <sup>37</sup>J. Pathak, B. Hunt, M. Girvan, Z. Lu, and E. Ott, “Model-free prediction of large spatiotemporally chaotic systems from data: A reservoir computing approach,” *Phys. Rev. Lett.* **120**, 024102 (2018).
- <sup>38</sup>Y. Tang, J. Kurths, W. Lin, E. Ott, and L. Kocarev, “Introduction to focus issue: When machine learning meets complex systems: Networks, chaos, and nonlinear dynamics,” *Chaos* **30**, 063151 (2020).
- <sup>39</sup>T. Arcmano, I. Szunyogh, J. Pathak, A. Wikner, B. R. Hunt, and E. Ott, “A machine learning-based global atmospheric forecast model,” *Geophys. Res. Lett.* **47**, e2020GL087776 (2020).
- <sup>40</sup>F. A. Rodrigues, T. K. D. Peron, C. Connaughton, J. Kurths, and Y. Moreno, “A machine learning approach to predicting dynamical observables from network structure,” (2019), preprint at <https://arxiv.org/abs/1910.00544> (2019).
- <sup>41</sup>H. Kim, D. Olave-Rojas, E. Álvarez-Miranda, and S.-W. Son, “In-depth data on the network structure and hourly activity of the Central Chilean power grid,” *Scientific data* **5**, 180209 (2018).
- <sup>42</sup>L. Pagnier and P. Jacquod, “Pantagruel - a pan-European transmission grid and electricity generation model,” (2019), <https://doi.org/10.5281/zenodo.2642175>.
- <sup>43</sup>“ENTSO-E transmission system map,” (2019), <https://www.entsoe.eu/data/map/>.
- <sup>44</sup>L. Hirth, J. Mühlenpfordt, and M. Bulkeley, “The ENTSO-E transparency platform - a review of europe’s most ambitious electricity data platform,” *Appl. Energy* **225**, 1054 (2018).
- <sup>45</sup>J. Machowski, Z. Lubosny, J. W. Bialek, and J. R. Bumby, *Power System Dynamics: Stability and Control*, 3rd ed. (John Wiley & Sons, Ltd., 2020).
- <sup>46</sup>A. Liaw and M. Wiener, “Classification and regression by randomForest,” *R News* **2**, 18 (2002).
- <sup>47</sup>L. Breiman, “Random forests,” *Mach. Learn.* **45**, 5 (2001).
- <sup>48</sup>C. Cortes and V. Vapnik, “Support-vector networks,” *Mach. Learn.* **20**, 273 (1995).
- <sup>49</sup>S. Amari and S. Wu, “Improving support vector machine classifier by modifying kernel functions,” *Neural Netw.* **12**, 783 (1999).
- <sup>50</sup>A. Géron, *Hands-On Machine Learning with Scikit-Learn and TensorFlow: Concepts, Tools, and Techniques to Build Intelligent Systems* (O’Reilly, 2017).
- <sup>51</sup>N. Srivastava, G. Hinton, A. Krizhevsky, I. Sutskever, and R. Salakhutdinov, “Dropout: a simple way to prevent neural networks from overfitting,” *J. Mach. Learn. Res.* **15**, 1929 (2014).
- <sup>52</sup>I. Goodfellow, Y. Bengio, and A. Courville, *Deep Learning* (MIT Press, 2016) <http://www.deeplearningbook.org>.
- <sup>53</sup>D. P. Kingma and J. L. Ba, “Adam: A method for stochastic optimizations,” (2017), preprint at <https://arxiv.org/abs/1412.6980v9> (2017).
- <sup>54</sup>F. Pedregosa, G. Varoquaux, A. Gramfort, V. Michel, B. Thirion, O. Grisel, M. Blondel, P. Prettenhofer, R. Weiss, V. Dubourg, J. Vanderplas, A. Passos, D. Cournapeau, M. Brucher, M. Perrot, Duchesnay, and Édouard, “Scikit-learn: Machine learning in python,” *J. Mach. Learn. Res.* **12**, 2825 (2011).
- <sup>55</sup>“scikit-learn: Machine Learning in Python,” (2020), <https://scikit-learn.org/stable/>. Accessed: 2020-01-09.
- <sup>56</sup>A. Paszke, S. Gross, F. Massa, A. Lerer, J. Bradbury, G. Chanan, T. Killeen, Z. Lin, N. Gimelshein, L. Antiga, *et al.*, “Pytorch: An imperative style, high-performance deep learning library,” (2019), preprint at <https://arxiv.org/abs/1912.01703> (2019).
- <sup>57</sup>“PyTorch,” (2019), <https://pytorch.org/docs/stable/>. Accessed: 2019-12-03.
- <sup>58</sup>M. E. J. Newman, *Networks*, 2nd ed. (Oxford University Press, 2018).
- <sup>59</sup>A.-L. Barabási, *Network science*, 1st ed. (Cambridge University Press, 2016).
- <sup>60</sup>H. Kim and S. H. Lee, “Relation flexibility of network elements based on inconsistent community detection,” *Phys. Rev. E* **100**, 022311 (2019).
- <sup>61</sup>A. Altmann, L. Toloşi, O. Sander, and T. Lengauer, “Permutation importance: a corrected feature importance measure,” *Bioinformatics* **26**, 1340 (2010).

<sup>62</sup>H. E. Nusse and J. A. Yorke, “Basin of attraction,” *Science* **271**, 1376 (1996).

<sup>63</sup>P. J. Menck, J. Heitzig, N. Marwan, and J. Kurths, “How basin stability complements the linear-stability paradigm,” *Nat. Phys.* **9**, 89 (2013).

<sup>64</sup>T. Nesti, F. Sloothaak, and B. Zwart, “Emergence of scale-free blackout sizes in power grids,” *Phys. Rev. Lett.* **125**, 058301 (2020).